A Unified Geometric Approach to Modeling and Control of Constrained Mechanical Systems

Guanfeng Liu and Zexiang Li, *Member, IEEE*

***Abstract*—Dynamic control of constrained mechanical systems, such as robotic manipulators under end-effector constraints, parallel manipulators, and multifingered robotic hands under closure constraints have been classic problems in robotics research. There have been numerous treatments on modeling, analysis, and control for each class of problem. In this paper, we provide a unified geometric framework for modeling, analysis, and control of constrained mechanical systems. Starting with the constraint, we define two canonical subspaces, namely the subspace of constraint forces and the tangent space of the constraint manifold for holonomic constraint. Using the kinetic energy metric, we define the remaining subspaces and show explicitly the relations among these subspaces. We project the Euler–Lagrange equation of a constrained mechanical system into two *orthogonal* components and give geometric and physical interpretations of the projected equations. Based on the projected equations, a unified and asymptotically stable hybrid position/force-control algorithm is proposed, along with experimental results for several practical examples. In the case of nonholonomic constraints, we show that the equations can be projected to the distribution/codistribution associated with the constraints and the control law reduces to hybrid velocity/force control.**

***Index Terms*—Asymptotic stability, constraints, distribution, hybrid control, projection, velocity and force.**

I. Introduction

CONTROL of constrained mechanical systems, such as manipulators with end-effector constraints, parallel manipulators, and multifingered robotic hands with closure constraints, have been classic problems in robotics research. Mason [1] introduced the notion of natural and artificial constraints and formalized a theoretical framework for compliant motion control. Based on Mason's work, Raibert and Craig [2] proposed a hybrid position/force control scheme.

Early work on hybrid control relied explicitly on identification of the force and velocity spaces using the usual inner product of $\mathbb{R}^6$ [3], [4]. The latter was, however, shown by Loncaric [5] and Duffy [4] to be neither coordinate invariant nor physically meaningful. Force and velocity are objects of different physical and geometric natures. As a matter of fact, the duality relation between force and velocity has long been recognized in [4], and [6]–[8]. Reciprocal product is used in some literature [6], [9] to express this duality relation. Based on this relation and the fact that constraint forces annihilating free velocities, Yoshikawa [10] presented a dynamic hybrid position/force-control algorithm. McClamroch [11] explicitly utilized the duality relation and the constraints to decouple the dynamics of constrained mechanical systems and develop a stable hybrid position/force-control algorithm. Selig [12] also used the duality relation to define two projection maps and gave a precise geometric interpretation of the constrained dynamics. Robustness issues of hybrid control algorithms, in regard to model uncertainties in manipulator dynamics and constraints, were discussed in [11] and [13]. A unified state space formulation for holonomic and nonholonomic systems was developed by Yun and Sarkar [14], which provided also a detailed discussion on how to eliminate the need to solve implicit functions. Closest to our current work is that of Blajer [15], [16], in which an elegant geometric treatment of constrained multibody dynamics was provided. Blajer proposed a novel projection scheme to decouple the constrained dynamics, and constructed covariant and contravariant bases to factorize the kinetic metric matrix and its inverse. This is, in fact, equivalent to the projection method in our current context. Much of the analysis presented here is based on developing suitable modifications and extensions to [16] for real applications involving control of constrained mechanical systems.

The theory of hybrid control has been exploited to model the dynamics and control of parallel manipulators [17], [18] and multifingered robotic hands in grasping and coordinated manipulation applications. Modeling of the latter system is usually performed by considering those constraints due to different types of contacts and friction cones in addition to loop-closure constraints [19]–[25]. It is also interesting to note that the procedure of obtaining the reduced dynamics through projection is not only applied to those systems with holonomic and nonholonomic constraints, but also to systems with symmetries [26], [27], as symmetries can be either modeled as a set of additional holonomic constraints or formulated as mechanical connections.

The goal of this paper is twofold. First, based on ideas from early papers [5], [9]–[13], [16], we present a precise geometric framework for hybrid control. Second, based on the geometric framework, we propose a simple hybrid control algorithm and prove its stability using a simple geometric argument. The geometric hybrid control theory we propose is widely applicable to not only manipulators with end-effector constraints (holonomic or nonholonomic), but also parallel manipulators and multifingered robotic hands with closure constraints.

The paper is organized as follows. In Section II, we use the constraint to define two natural subspaces, the constraint force

Manuscript received May 28, 2001; revised December 26, 2001. This paper was recommended for publication by Associate Editor S. Chiaverini and Editor A. De Luca upon evaluation of the reviewers' comments.

The authors are with the Department of Electrical and Electronic Engineering, Hong Kong University of Science and Technology, Kowloon, Hong Kong (e-mail: liugf@ust.hk; eezxli@ust.hk).

Digital Object Identifier 10.1109/TRA.2002.802207

subspace in the cotangent space and the free (or constrained) velocity subspace in the tangent space. The kinetic energy metric of the system helps to define the remaining subspaces. Two projection maps are then defined using the metric and the constraint. The Euler–Lagrange equation of the constrained system is decomposed into two parts using the projection maps. Geometric interpretations of the two component equations in terms of the curvature of the constraint submanifold are provided. In Section III, based on the geometric structure of the dynamic equations, a modified computed-torque type algorithm is proposed for hybrid position/force control. Asymptotic stability of the closed-loop system is proved using the decoupled nature of the error dynamics. For nonholonomic systems, this control law reduces to hybrid velocity/force control. In Section IV, several practical examples are studied in detail along with experimental results, showing validity and simplicity of the proposed control algorithm. Section V concludes the paper with several important remarks.

II. Geometric Model of Constrained Mechanical Systems

This section develops a unified geometric model for constrained mechanical systems, including robotic manipulators with end-effector constraints, parallel manipulators, and multifingered robotic hands with closure constraints. Constraints here are introduced either because of interaction of the system with its environment, parallel structures of the system, or a combination of both, such as manipulating an object by a multifingered robotic hand. Readers are referred to [9] and [28]–[32] for more detailed treatment of some geometric concepts used here.

A. Geometry of the Constraint Submanifold

Let E be the configuration space of an (unconstrained) mechanical system, and $\theta \in \mathbb{R}^n$ its local (or generalized) coordinates. The tangent space to E at θ, denoted $T_\theta E$, consists of all velocity vectors of the system, and the cotangent space to E at θ, denoted $T_\theta{}^*E$, consists of all (generalized) force vectors. A (generalized) force vector $\alpha \in T_\theta^* E$ is also referred to as a covector. It pairs with a vector $v \in T_\theta E$ to produce a real number $\langle \alpha, v \rangle$. For instance, let $E = \mathbb{S}^1 \times \cdots \times \mathbb{S}^1$, the joint space of an open-chain manipulator. Then, $\dot\theta \in T_\theta E$, $\tau \in T_\theta^* E$, and $\langle \tau, \dot\theta \rangle$ is the virtual work done by τ on $\dot\theta$. As another example, let $E = SE(3)$, the configuration space of a rigid body. Then, $T_g SE(3)$ can be identified with the Lie algebra $se(3)$ via left translation and $T_g^* SE(3)$ with $se^*(3)$. An element $\xi \in se(3)$ can be written as $\xi = (v, w) \in \mathbb{R}^6$, and an element F of $se^*(3)$ as $F = (f, m)$. The pairing between F and ξ is given by $\langle F, \xi \rangle = f^T \cdot v + m^T \cdot w$.

Definition 1: Constraint: A constraint on a mechanical system E is a relation of the form

$$\begin{bmatrix} a_1^T(\theta) \\ \vdots \\ a_{n-m}^T(\theta) \end{bmatrix} \dot\theta := A(\theta)\dot\theta = 0, \quad \forall \dot\theta \in T_\theta E \tag{1}$$

where $(a_i(\theta))_{i=1}^{n-m} \in T_\theta^* E$ are referred to as the constraint forces.

A constraint is said to be well defined if it is associated with physically realizable constraint forces. The physical constraints described in [1] are well defined, but not the artificial constraints or the virtual constraints as in [12]. The latter should be modeled rather as position or velocity control objectives. Without loss of generality, we shall assume that the constraint forces are linearly independent. A constraint is said to be holonomic or integrable if there exist $(n-m)$ real-valued functions $h_i(\theta), i = 1, \ldots, n-m$ such that $\partial h_i / \partial \theta = a_i(\theta)$. In this case, the constraint can be rewritten as $h_i(\theta) = c_i$ for some constant $c_i, i = 1, \ldots, n-m$. Define

$$H : E \longrightarrow \mathbb{R}^{n-m}, H(\theta) = (h_1(\theta), \ldots h_{n-m}(\theta))^T.$$

Then, the m-dimensional submanifold $Q = H^{-1}(c)$ is referred to as the configuration space of the constrained system, with E being its ambient space. At each $\theta \in Q$, the tangent space of Q, $T_\theta Q$, defines the set of allowed velocities of the constrained system, and the set of constraint forces, defined by

$$T_\theta^* Q^\perp = \{ f \in T_\theta^* E \mid \langle f, v \rangle = 0, \forall v \in T_\theta Q \}$$

are spanned by $a_i(\theta), i = 1, \ldots n-m$.

Let $\mathcal{K} = (1/2)\dot\theta^T M(\theta)\dot\theta$ be the kinetic energy of the mechanical system. It endows $T_\theta E$ with a natural Riemannian metric M. Using this metric, the orthogonal complement of $T_\theta Q$ can be defined [33]

$$T_\theta Q^\perp = \left\{ v_1 \in T_\theta E \mid \langle\langle v_1, v_2 \rangle\rangle_M = v_1^T M v_2 = 0, \forall v_2 \in T_\theta Q \right\}$$

and the cotangent space $T_\theta^* Q$ consists of covectors which annihilate vectors in $T_\theta Q^\perp$

$$T_\theta^* Q = \left\{ f \in T_\theta^* E \mid \langle f, v \rangle = 0, \forall v \in T_\theta Q^\perp \right\}.$$

To summarize, we have a (holonomically) constrained system (E, A) that is naturally associated with two subspaces $T_\theta Q$ and $T_\theta^* Q^\perp$. If the system is further endowed with a kinetic-energy metric M, then two additional subspaces $T_\theta Q^\perp$ and $T_\theta^* Q$ can be defined. The velocity and force spaces therefore split according to

$$\begin{aligned} T_\theta E &= T_\theta Q \oplus T_\theta Q^\perp \\ T_\theta^* E &= T_\theta^* Q \oplus T_\theta^* Q^\perp. \end{aligned}$$

Note that the metric M allows us to identify the tangent space with the cotangent space,

$$M^\flat : T_\theta E \to T_\theta^* E : \left\langle M^\flat v_1, v_2 \right\rangle = v_1^T M v_2.$$

As M is positive definite, $M^\flat$ has an inverse, denoted by $M^\sharp$. It is not difficult to see that the matrix representation of $M^\flat$ is simply M, and that of $M^\sharp$ is M^{-1}. Also, observe that

$$M^\sharp (T_\theta^* Q) = T_\theta Q \quad \text{and} \quad M^\sharp \left(T_\theta^* Q^\perp \right) = T_\theta Q^\perp.$$

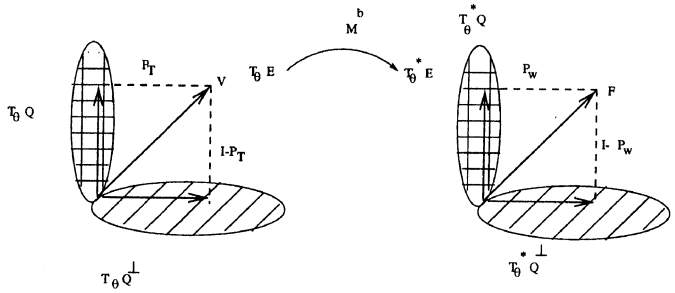

Fig. 1. Geometric relations among the four defined subspaces.

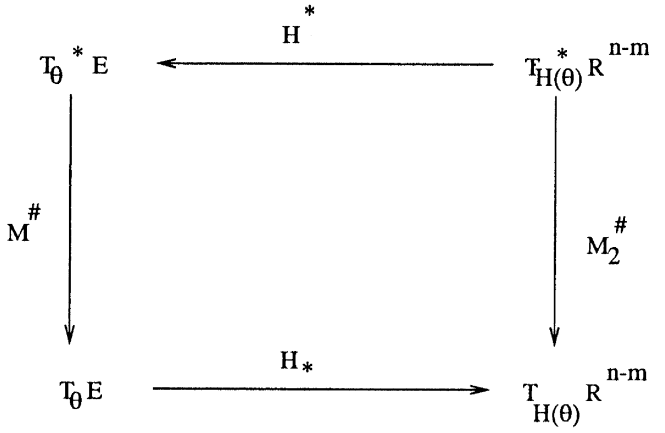

Fig. 2. Commutative diagram for the four defined subspaces.

In other words, constraint forces can be identified with velocities orthogonal to the free velocities provided there is a nonsingular metric. Fig. 1 summarizes the relations between the four subspaces. Let

$$H_*: T_\theta E \longrightarrow T_{H(\theta)}\mathbb{R}^{n-m} \text{ and } H^*: T^*_{H(\theta)}\mathbb{R}^{n-m} \longrightarrow T^*_\theta E$$

be, respectively, the tangent map of H and its dual. The null space of H_* is exactly $T_\theta Q$. Thus, H_* identifies $T_\theta Q^\perp$ with $T_{H(\theta)}\mathbb{R}^{n-m}$, and H^* identifies $T^*_{H(\theta)}\mathbb{R}^{n-m}$ with ${T_\theta}^* Q^\perp$. From the commutative diagram in Fig. 2, we can identify $T^*_{H(\theta)}\mathbb{R}^{n-m}$ with $T_{H(\theta)}\mathbb{R}^{n-m}$ by

$$M_2^\sharp := H_* M^\sharp H^*.$$

Lemma 1: The map $(I - P_w): T^*_\theta E \longrightarrow T^*_\theta Q^\perp$, given by

$$(I - P_w) = H^* M_2^\flat H_* M^\sharp$$

is a well-defined projection map, with the property that $(I - P_w) f_1 = 0, \forall f_1 \in T^*_\theta Q$, and $(I - P_w) f_2 = f_2, \forall f_2 \in T^*_\theta Q^\perp$.

Proof: Given $f_1 \in T^*_\theta Q$, we have $M^\sharp(f_1) \in T_\theta Q = \eta(H_*)$ and thus, $(I - P_w)(f_1) = 0$. On the other hand, for $f_2 \in T^*_\theta Q^\perp$, there exists $\lambda \in \mathbb{R}^{n-m}$ such that $f_2 = H^*\lambda$ and

$$(I - P_w) f_2 = H^* M_2^\flat H_* M^\sharp H^* \lambda = H^* \lambda = f_2.$$

This also shows that $P_w: T^*_\theta E \to T^*_\theta Q$ is a well-defined projection map. In a similar manner, we define the projection map in the tangent spaces, $P_T: T_\theta E \longrightarrow T_\theta Q$, by

$$P_T = I - M^\sharp H^* M_2^\flat H_*$$

and $(I - P_T): T_\theta E \longrightarrow T_\theta Q^\perp$, the projection map to $T_\theta Q^\perp$. These projection maps are depicted in Fig. 1.

Lemma 2: P_T and P_w have the following properties:

$$\begin{aligned} P_w M &= M P_T \\ P_w H^* &= H_* P_T = 0 \\ P_T &= P_w^T. \end{aligned}$$

When the constraint is nonholonomic, the set of free velocities define a distribution $\Delta_\theta \subset T_\theta E$, and the set of constraint forces define a codistribution $\Delta^{*\perp}_\theta \subset T^*_\theta E$. The corresponding projection maps are defined by simply replacing H_* with A and H^* with A^T.

Remark 1: The symbols $\sharp$ and $\flat$ associated with the identification map between the tangent space and the cotangent space are standard in the literature of mechanics [34].

Remark 2: Although we assume the constraints in (1) are scleronomic, the developed framework can also be applied to systems with rheonomic (nonscleronomic) constraints.

B. Euler–Lagrange Equations of Constrained Systems: A Geometric View

In this subsection, we use the two projection maps to give a geometric interpretation of the projected dynamics of a constrained mechanical system. The results will be subsequently used in the derivation of stable hybrid control laws.

For a mechanical system with kinetic energy $\mathcal{K} = (1/2)\dot\theta^T M(\theta)\dot\theta$, potential energy $\mathcal{V}(\theta)$ and constraint given in (1), the general form of equations of motion is [9]

$$\frac{d}{dt}\left(\frac{\partial L}{\partial \dot\theta}\right) - \frac{\partial L}{\partial \theta} = \tau + A^T\lambda \tag{2}$$

where $L = \mathcal{K} - \mathcal{V}$ is the Lagrangian function, $\lambda \in \mathbb{R}^{n-m}$ the Lagrange multipliers, and $\tau \in \mathbb{R}^n$ the joint torque vector (some components may be zero in the case of parallel manipulators and robotic hands). The above equations can be manipulated into the form

$$M\ddot\theta + C\left(\theta, \dot\theta\right) + N = \tau + A^T\lambda \tag{3}$$

with C denoting the centrifugal and Coriolis forces and N the gravitational force.

Differentiating the constraint (1) and eliminating $\ddot\theta$ from (3), we have

$$\lambda = \left(AM^{-1}A^T\right)^{-1}\left(-\dot A\dot\theta + AM^{-1}(C + N - \tau)\right). \tag{4}$$

Substituting (4) back to (3) yields

$$M\ddot\theta + A^T\left(AM^{-1}A^T\right)^{-1}\dot A\dot\theta + P_w C + P_w N = P_w\tau \tag{5}$$

where

$$P_w = I - A^T\left(AM^{-1}A^T\right)^{-1}AM^{-1}$$

is the projection map from $T^*_\theta E$ to $T^*_\theta Q$ defined previously. Let $\tilde C = P_w C$, $\tilde N = P_w N$, and $\tilde\tau = P_w\tau$ be, respectively, the projection of C, N, and τ to $T^*_\theta Q$. The first two terms in the

left-hand side of (5) are seen to have the following interesting interpretations

$$M\ddot{\theta} + A^T \left(AM^{-1}A^T\right)^{-1} \dot{A}\dot{\theta} = P_w M\ddot{\theta} := \tilde{M}\ddot{\theta}$$

with $\tilde{M}\ddot{\theta}$ understood as the inertia force in $T^*_\theta Q$. Thus, the projected dynamics in $T^*_\theta Q$ are given by

$$\boxed{\tilde{M}\ddot{\theta} + \tilde{C} + \tilde{N} = \tilde{\tau}.} \tag{6}$$

To project the dynamics to $T^*_\theta Q^\perp$, we apply the projection map $(I - P_w)$ to (3) and realize that the constraint force already lies in $T^*_\theta Q^\perp$

$$(I - P_w)\left(M\ddot{\theta} + C + N\right) = (I - P_w)\tau + A^T\lambda. \tag{7}$$

If we let

$$P_T = I - M^{-1}A^T \left(AM^{-1}A^T\right)^{-1} A$$

be the projection map from $T_\theta E$ to $T_\theta Q$, and utilize the property that $P_w M = M P_T$, we have

$$\boxed{M\left(I - P_T\right)\left(\ddot{\theta} + M^{-1}C\right) = (I - P_w)(\tau - N) + A^T\lambda.} \tag{8}$$

C. Reduced Dynamics and Second Fundamental Form

Using the language of connections in Riemannian manifold [28], we can give a deeper geometric understanding of (6) and (8). First, denote by ∇ the affine connection compatible with the Riemannian metric M. Then the Euler–Lagrange (3) can be rewritten as [35]

$$M\nabla_{\dot{\theta}}\dot{\theta} = \tau - N + A^T\lambda. \tag{9}$$

Given tangent vector fields X, Y to the submanifold Q, $\nabla_X Y$ is the covariant derivative of Y in the direction X. Usually, $\nabla_X Y$ is not necessary tangent to Q, but it can be decomposed into a term that is tangent to Q and a term that is normal to Q. Let $\tilde{\nabla}$ be the induced connection on Q by ∇ (i.e., $\tilde{\nabla}$ is the connection of Q that is compatible to the induced metric on Q) and

$$S : \mathcal{T}(Q) \otimes \mathcal{T}(Q) \to \mathcal{N}(Q)$$

the second fundamental form (or extrinsic curvature form) of Q, where $\mathcal{T}(Q)$ and $\mathcal{N}(Q)$ are, respectively, the set of tangent and normal vector fields of Q. Then

$$\nabla_X Y = \tilde{\nabla}_X Y + S(X, Y).$$

Thus, the term $(I - P_T)(\ddot{\theta} + M^{-1}C)$ in (8) is interpreted as the second fundamental form $S(\dot{\theta}, \dot{\theta})$ for the constraint submanifold Q for $\dot{\theta} \in T_\theta Q$, and $MS(\dot{\theta}, \dot{\theta})$ is viewed as the centrifugal force due to the curvature of Q in its ambient space (or extrinsic curvature). Consequently, (6) becomes

$$\boxed{M\tilde{\nabla}_{\dot{\theta}}\dot{\theta} = \tilde{\tau} - \tilde{N}} \tag{10}$$

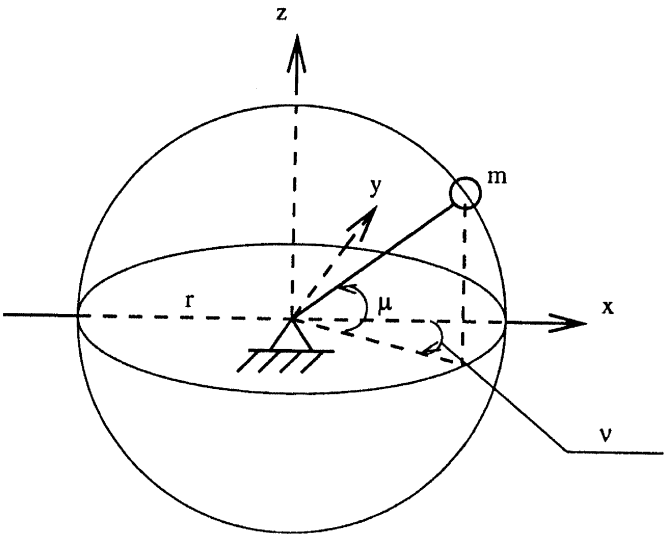

Fig. 3. Spherical pendulum.

and (8) assumes the more compact form

$$\boxed{MS\left(\dot{\theta}, \dot{\theta}\right) = (I - P_w)(\tau - N) + A^T\lambda.} \tag{11}$$

Equations (10) and (11) are very important in the development of stable hybrid position/force-control algorithms for holonomic systems. When the constraint is nonholonomic, we will rely on (6) and (8), where the term $(I - P_T)(\ddot{\theta} + M^{-1}C)$ can still be interpreted as the component of the acceleration $\nabla_{\dot{\theta}}\dot{\theta}$ in $\Delta^\perp_p$, and $M(I - P_T)(\ddot{\theta} + M^{-1}C)$ is to be regarded as the centrifugal force due to the fact that the distribution Δ is nonparallel.

Example 1: Dynamics of a Spherical Pendulum: Consider the motion of a spherical pendulum with mass m, as shown in Fig. 3. The kinetic energy of the pendulum is given by

$$\mathcal{K} = \frac{1}{2}m\left(\dot{x}^2 + \dot{y}^2 + \dot{z}^2\right) := \frac{1}{2}\dot{\theta}^T M\dot{\theta}$$

where $\theta = (x, y, z)^T$ and $M = mI$. The constraint is given by

$$\theta^T\theta - r^2 = 0$$

from which we have $A = (x, y, z)$ and $M_2^\sharp = AM^\sharp A^T = r^2/m$. The projection map P_w and $I - P_w$ are calculated as

$$P_w = \frac{1}{r^2}\begin{bmatrix} y^2 + z^2 & -xy & -xz \\ -yx & x^2 + z^2 & -yz \\ -zx & -zy & x^2 + y^2 \end{bmatrix}$$

and

$$I - P_w = \frac{1}{r^2}\begin{bmatrix} x^2 & xy & xz \\ yx & y^2 & yz \\ zx & zy & z^2 \end{bmatrix}.$$

From *Lemma 2*, $P_T = P_w^T = P_w$. Let us denote by ∇ the Riemannian connection compatible with M. We have $\nabla_{\dot{\theta}}\dot{\theta} = \ddot{\theta}$. Let (μ, ν) be the spherical coordinates and

$\theta = (r\cos\mu\cos\nu, r\cos\mu\sin\nu, r\sin\mu)^T$. The induced connection and the second fundamental form can be computed by applying the two projection maps

$$\begin{aligned}\tilde{\nabla}_{\dot\theta}\dot\theta &= P_T\left(\nabla_{\dot\theta}\dot\theta\right)\\ &= \begin{bmatrix} -r\sin\mu\cos\nu & -r\sin\nu \\ -r\sin\mu\sin\nu & r\cos\nu \\ r\cos\mu & 0 \end{bmatrix}\begin{bmatrix} v_1 \\ v_2 \end{bmatrix} \qquad (12)\\ S\left(\dot\theta,\dot\theta\right) &= (I-P_T)\left(\nabla_{\dot\theta}\dot\theta\right)\\ &= \left(-\dot\mu^2-\cos^2\mu\dot\nu^2\right)\begin{bmatrix} r\cos\mu\cos\nu \\ r\cos\mu\sin\nu \\ r\sin\mu \end{bmatrix} \qquad (13)\end{aligned}$$

where $v_1 = \ddot\mu + \sin\mu\cos\mu\dot\nu^2$ and $v_2 = \cos\mu\ddot\nu - 2\sin\mu\dot\mu\dot\nu$. One remarkable property of the second fundamental form $S(\dot\theta,\dot\theta)$ is that it only depends on the first-order derivative of local coordinates. In fact, we can also deduce the expression of $\tilde\nabla_{\dot\theta}\dot\theta$ directly from the induced metric $\tilde M$, given by

$$\begin{bmatrix} r^2 & 0 \\ 0 & r^2\cos^2\mu \end{bmatrix}.$$

The Christoffel symbols of $\tilde\nabla$ are computed as

$$\begin{aligned}\Gamma^\mu_{\mu\mu} &= 0, \quad \Gamma^\nu_{\mu\mu} = 0\\ \Gamma^\mu_{\mu\nu} &= 0, \quad \Gamma^\nu_{\mu\nu} = -\frac{\sin\mu}{\cos\mu}\\ \Gamma^\mu_{\nu\mu} &= 0, \quad \Gamma^\nu_{\nu\mu} = -\frac{\sin\mu}{\cos\mu}\\ \Gamma^\mu_{\nu\nu} &= \sin\mu\cos\mu, \quad \Gamma^\nu_{\nu\nu} = 0.\end{aligned}$$

Let $\dot\theta = \dot\mu\partial/\partial\mu + \dot\nu\partial/\partial\nu$, we have

$$\tilde\nabla_{\dot\theta}\dot\theta = \left(\ddot\mu + \sin\mu\cos\mu\dot\nu^2\right)\frac{\partial}{\partial\mu} + \left(\ddot\nu - 2\frac{\sin\mu}{\cos\mu}\dot\mu\dot\nu\right)\frac{\partial}{\partial\nu} \qquad (14)$$

where

$$\begin{aligned}\frac{\partial}{\partial\mu} &= (-r\sin\mu\cos\nu, -r\sin\mu\sin\nu, r\cos\mu)^T\\ \frac{\partial}{\partial\nu} &= (-r\cos\mu\sin\nu, r\cos\mu\cos\nu, 0)^T.\end{aligned}$$

Note that (12) and (14) give the same results.

III. Unified Hybrid-Control Algorithm for Constrained Systems

Based on (6) and (8), we propose in this section a unified hybrid-control algorithm for constrained mechanical systems. When the constraint is holonomic, the algorithm achieves hybrid position/force control, and hybrid velocity/force control when the constraint is nonholonomic. Using the decoupled nature of these two equations, we give a simple asymptotic stability proof of the control algorithms.

A. Hybrid Position/Force Control for Holonomic Systems

When the constraint in (1) is holonomic, it defines a m-dimensional submanifold Q in E. Let $\tilde\theta \in \mathbb{R}^m$ be the local coordinates of Q, and $\theta = \psi(\tilde\theta)$ the corresponding embedding of Q in E. Denote by J the Jacobian matrix of ψ, i.e.

$$\dot\theta = J\dot{\tilde\theta} \quad \text{and} \quad \ddot\theta = J\ddot{\tilde\theta} + \dot J\dot{\tilde\theta}.$$

Substituting the above expressions into (3) yields

$$MJ\ddot{\tilde\theta} + C_1 + N = \tau + A^T\lambda \qquad (15)$$

where $C_1 = M\dot J\dot{\tilde\theta} + C(\psi(\tilde\theta), J\dot{\tilde\theta})$. Applying the two projection maps P_w and $I - P_w$ from the previous section to (15) gives the decoupled dynamics

$$P_wMJ\ddot{\tilde\theta} + P_w(C_1 + N) = P_w\tau \qquad (16)$$

and

$$(I-P_w)MJ\ddot{\tilde\theta} + (I-P_w)(C_1+N) = (I-P_w)\tau + A^T\lambda. \qquad (17)$$

Since Image$(J) = T_\theta Q$, $M(T_\theta Q) = T^*_\theta Q$, and $I - P_w$ is a projection map onto $T^*_\theta Q^\perp$, we conclude that $(I-P_w)MJ = 0$ and $MS(\dot\theta,\dot\theta) = (I-P_w)(M\ddot\theta + C) = (I-P_w)C_1$. We propose the following control algorithm for the above equations:

$$P_w\tau = P_wMJ\left(\ddot{\tilde\theta}_d - K_v\dot{\tilde e} - K_p\tilde e\right) + P_w(C_1+N) \qquad (18)$$

and

$$\begin{aligned}(I-P_w)\tau &= (I-P_w)(C_1+N)\\ &\quad + A^T\left(-\lambda_d + K_I\int(\lambda-\lambda_d)\right)\end{aligned} \qquad (19)$$

where $\tilde e = \tilde\theta - \tilde\theta_d$ is the position trajectory tracking error, K_v, $K_p \in \mathbb{R}^{m\times m}$ the velocity and position feedback gains, $\lambda_d = (AA^T)^{-1}Af_d$ with f_d the desired constraint force, and $K_I \in \mathbb{R}^{(n-m)\times(n-m)}$ the integral force gain. λ is computed from the actual constraint force, which, in turn, is obtained by projecting the force sensed by the (wrist) force/torque sensor to the constraint force space. Note that $P_w\tau$ consists of a feedback term and a feedforward term, which compensates the dynamics in the cotangent space of Q. On the other hand, the feedforward term of $(I-P_w)\tau$ is used to compensate the dynamics, due to the second fundamental form of Q. Combining the above expressions gives the total control law for τ

$$\begin{aligned}\tau &= MJ\left(\ddot{\tilde\theta}_d - K_v\dot{\tilde e} - K_p\tilde e\right) + C_1 + N\\ &\quad + A^T\left(-\lambda_d + K_I\int(\lambda-\lambda_d)\right).\end{aligned} \qquad (20)$$

B. Hybrid Velocity/Force Control for Nonholonomic Systems

When the constraint in (1) is nonholonomic, it defines a nonintegrable distribution Δ_θ in TE. There exists no manifold Q with the property that $T_\theta Q = \Delta_\theta$ for all $\theta \in Q$, and it is meaningless to talk about hybrid position/force control. The problem can be remedied, however, by introducing hybrid velocity/force control. For this, let $J(\theta) \in \mathbb{R}^{n\times m}$ be such that its columns span

Δ_θ, i.e., $AJ = 0$, and express $\dot\theta$ as $\dot\theta = Ju$ for some function u. Substituting $\ddot\theta = J\dot u + \dot J u$ into (3) yields

$$MJ\dot u + \left(M\dot J u + C\right) + N = \tau + A^T\lambda.$$

Similar to the case of holonomic systems, we propose the following control law for nonholonomic systems:

$$\tau = MJ\left(\dot u_d - K_p\left(u - u_d\right)\right) + \left(M\dot J u + C\right) + N + A^T\left(-\lambda_d + K_I\int\left(\lambda - \lambda_d\right)\right). \quad (21)$$

C. Stability Analysis

First, consider the holonomic case with the control law given by (20) and the error dynamics by

$$J\left(\ddot{\tilde e} + K_v\dot{\tilde e} + K_p\tilde e\right) = M^{-1}A^T\cdot\left(\lambda - \lambda_d + K_I\int\left(\lambda - \lambda_d\right)\right). \quad (22)$$

As explained previously, the column vectors of J and $M^{-1}A^T$ are perpendicular, i.e.

$$J^TM\left(M^{-1}A^T\right) = 0.$$

Therefore, the coefficients in both sides of (22) are zero

$$\ddot{\tilde e} + K_v\dot{\tilde e} + K_p\tilde e = 0$$
$$\left(\lambda - \lambda_d\right) + K_I\int\left(\lambda - \lambda_d\right) = 0.$$

If the feedback gains K_v, K_p, and K_I are chosen to be positive definite, then both position and force trajectory tracking errors converge to zero as t goes to infinity. This shows that orthogonality of the two subspaces, $T_\theta Q$ and $T_\theta Q^\perp$, leads to full decoupling of the position and force errors dynamics and, consequently, asymptotic stability of the feedback system. Observe that the error dynamics given here are different from that of [11] and [36 (4.108–4.109, Ch. 4.3, pp. 163)]. In a similar manner, we show that the error dynamics for a nonolonomic system with control law given in (21) are of the form

$$\left(\dot u_d - \dot u\right) + K_p\left(u - u_d\right) = 0$$
$$\left(\lambda - \lambda_d\right) + K_I\int\left(\lambda - \lambda_d\right) = 0.$$

Thus, with stable K_p and K_I, both velocity and force errors go to zero.

Remark 3: Decoupling between the position and force error dynamics is achieved here with a positive-definite matrix M. M can be the inertia matrix of the system or some other nondegenerate metrics, giving possibilities for the design of other control algorithms.

IV. Examples

In this section, we present several examples to illustrate the geometric hybrid control theory of the previous sections.

Example 2: A Two-Degree-of-Freedom (DOF) Cartesian Robot Moving on an Ellipse: Fig. 4 shows a Cartesian robot constrained to move on an ellipse. The forward kinematics of the manipulator is trivially

$$x(\theta) = x_0 + \theta_1$$
$$y(\theta) = y_0 + \theta_2$$

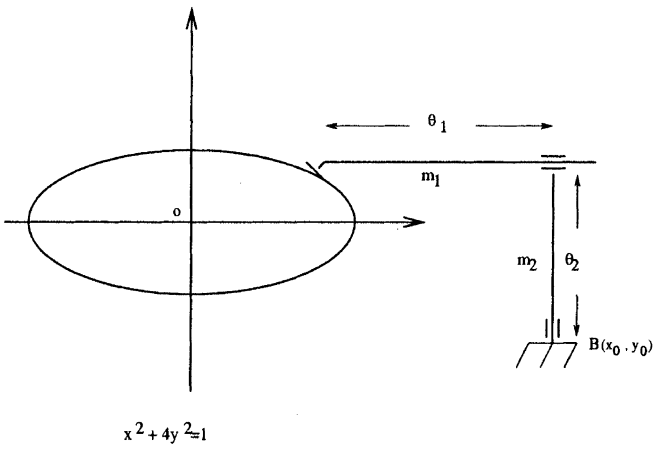

Fig. 4. A two-DOF manipulator following an ellipse.

and the constraint is given by

$$\left(x_0 + \theta_1\right)^2 + 4\left(y_0 + \theta_2\right)^2 - 1 = 0.$$

Thus, $A = (x_0 + \theta_1, 4(y_0 + \theta_2))$. The dynamic equation of the manipulator is

$$\begin{bmatrix} m_1 & 0 \\ 0 & m_1 + m_2 \end{bmatrix}\begin{bmatrix}\ddot\theta_1 \\ \ddot\theta_2\end{bmatrix} = \begin{bmatrix}\tau_1 \\ \tau_2\end{bmatrix} + \begin{bmatrix} x_0 + \theta_1 \\ 4\left(y_0 + \theta_2\right)\end{bmatrix}\lambda.$$

The two projection maps P_w and $(I - P_w)$ are calculated as

$$P_w = \alpha\begin{bmatrix} 16m_1y^2 & -4m_1xy \\ -4\left(m_1 + m_2\right)xy & \left(m_1 + m_2\right)x^2\end{bmatrix}$$
$$\left(I - P_w\right) = \alpha\begin{bmatrix}\left(m_1 + m_2\right)x^2 & 4m_1xy \\ 4\left(m_1 + m_2\right)xy & 16m_1y^2\end{bmatrix}$$

where $\alpha = 1/((m_1 + m_2)x^2 + 16m_1y^2)$. Assuming that $y \neq 0$, the projected equations in terms of the θ_1 coordinate are

$$\frac{1}{4\alpha}\ddot\theta_1 + \frac{\left(m_1 + m_2\right)x}{16y^2}\dot\theta_1^2 = 4y^2\tau_1 - xy\tau_2$$
$$-\frac{x}{4y}\dot\theta_1^2 - \frac{1}{m_1\left(m_1 + m_2\right)\alpha}x\lambda = \frac{x^2}{m_1}\tau_1 + \frac{4xy}{m_1 + m_2}\tau_2.$$

The control law is of the form

$$\tau_1 = m_1\left(\ddot\theta_{1d} - K_v\dot{\tilde e} - K_p\tilde e\right) + x\left(-\lambda_d + K_I\int\left(\lambda - \lambda_d\right)\right) \quad (23)$$

$$\tau_2 = -\frac{\left(m_1 + m_2\right)x}{4y}\left(\ddot\theta_{1d} - K_v\dot{\tilde e} - K_p\tilde e\right) - \frac{1}{16y^3}\left(m_1 + m_2\right)\dot\theta_1^2 + 4y\left(-\lambda_d + K_I\int\left(\lambda - \lambda_d\right)\right). \quad (24)$$

Fig. 5 shows the simulated position and force responses for the following parameters: $m_1 = m_2 = 1$ kg, $K_p = 3$, $K_v = 3$, and $K_I = 1$. The initial positions are $x = 0.5$ m and $y = 0.433$ m, with $x_0 = 2.0$ m and $y_0 = 1.0$ m.

Example 3: A Six-DOF Manipulator Moving on a Sphere With Frictionless Point Contact: Fig. 6 shows a six-DOF manipulator that is constrained to slide on a sphere with frictionless point contact. The end-effector is required to be normal to the sphere (*artificial constraint*). Following the notations in [9] and

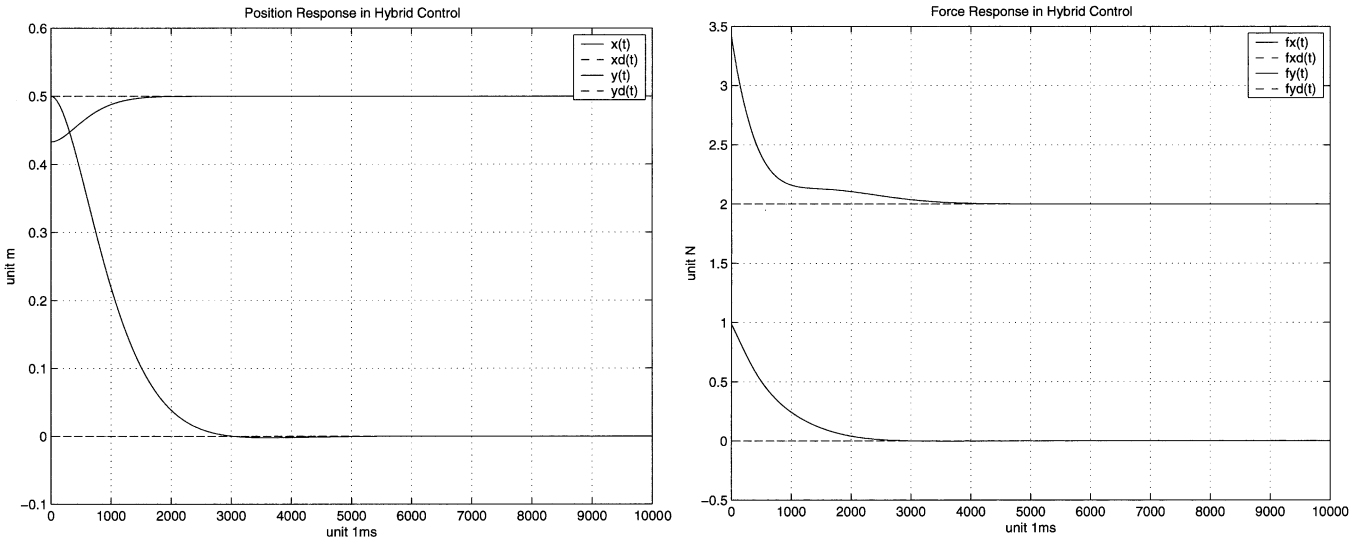

Fig. 5. Simulated position and force responses for *Example 2*.

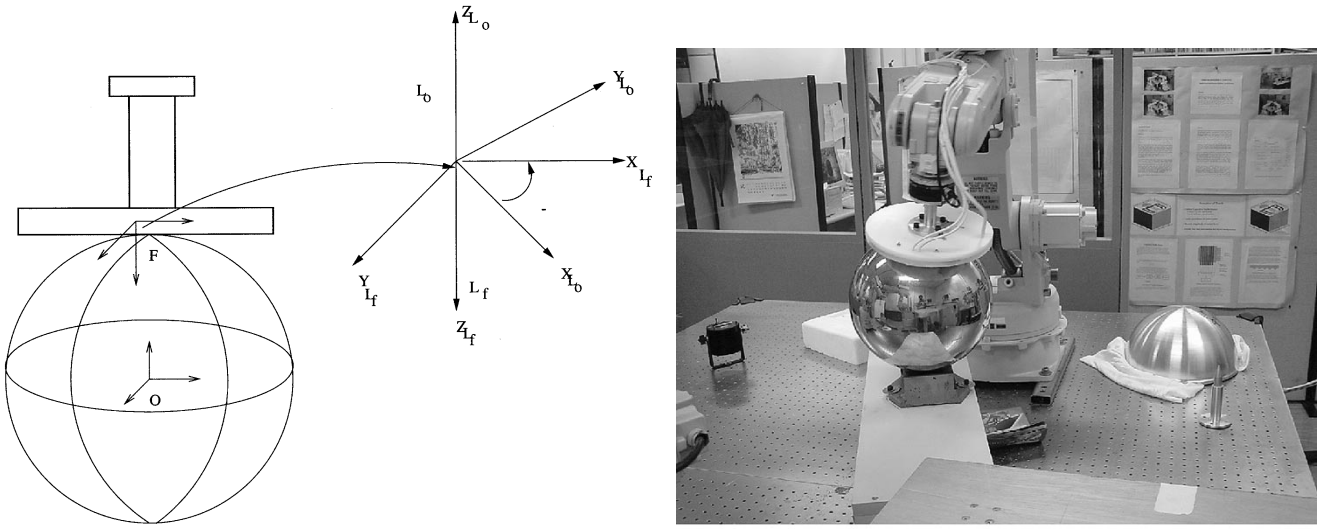

Fig. 6. A six-DOF manipulator moving on a sphere with frictionless point contact.

[37], let F and O be the reference frames of the end-effector and the object, respectively, and L_f and L_o their local frames at the point of contact. The configuration space of the system is the Euclidean group $SE(3)$, represented by the position and orientation of F with respect to O. Contact constraint in terms of the velocity $V_{l_o l_f} = (v_x, v_y, v_z, w_x, w_y, w_z)^T$ of the local frames is simply

$$v_z = 0 \quad \text{or} \quad [0 \quad 0 \quad 1 \quad 0 \quad 0 \quad 0] Ad_{g_{fl_f}^{-1}} V_{of} = 0.$$

Without loss of generality, we further assume that $g_{fl_f} = I$ and thus, $A = [0 \quad 0 \quad 1 \quad 0 \quad 0 \quad 0]$. This constraint is found to be holonomic [38], and its integral submanifold is the five-dimensional contact space Q that can be parameterized by Montana's contact coordinates $\eta = (\alpha_o^T, \alpha_f^T, \psi)^T$, where $\alpha_o = (u_o, v_o)^T$ is the coordinates of contact for the sphere, $\alpha_f = (u_f, v_f)^T$ the coordinates of contact for the end-effector, and ψ the angle of contact. We parameterize the sphere by the longitude and latitude angles and the end-effector the plane coordinates. The geometric parameters of the sphere and the end-effector in terms of these parameterizations are given by

$$M_o = \begin{bmatrix} \rho & 0 \\ 0 & \rho \cos u_o \end{bmatrix}, \; K_o = \begin{bmatrix} \frac{1}{\rho} & 0 \\ 0 & \frac{1}{\rho} \end{bmatrix},$$
$$T_o = \begin{bmatrix} 0 & -\frac{1}{\rho} \tan u_o \end{bmatrix}$$

and

$$M_f = \begin{bmatrix} 1 & 0 \\ 0 & 1 \end{bmatrix}, \; K_f = \begin{bmatrix} 0 & 0 \\ 0 & 0 \end{bmatrix},$$
$$T_f = [0 \quad 0].$$

Let $M = \text{diag}(m, m, m, I_x, I_y, I_z)$ be the inertia tensor of the end-effector. The projection maps are found to be

$$P_w = \text{diag}(1, 1, 0, 1, 1, 1) \text{ and } I - P_w = \text{diag}(0, 0, 1, 0, 0, 0).$$

Let $F_m \in \mathbb{R}^6$ be the force exerted on the end-effector by the manipulator and G the gravitational force. The Newton-Euler

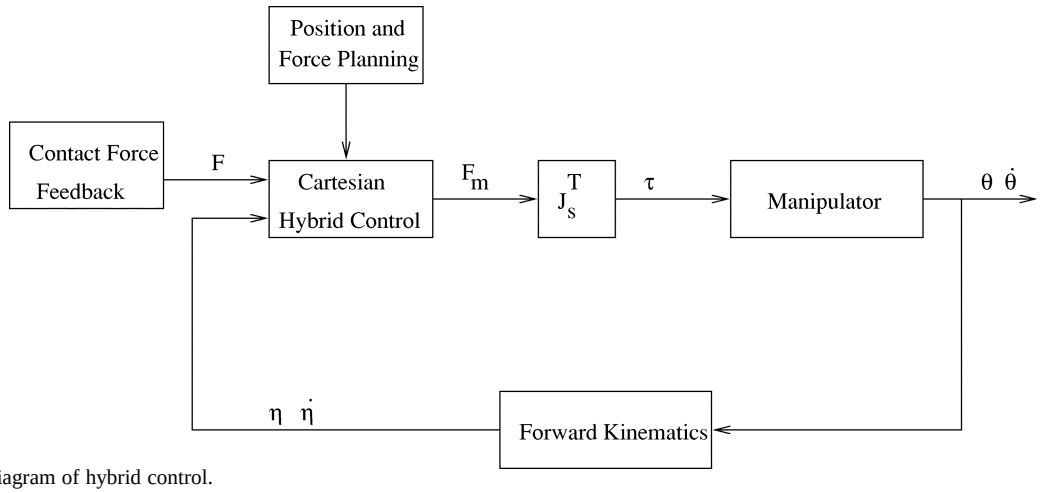

Fig. 7. Control diagram of hybrid control.

equation of motion for the end-effector admits a coordinate-invariant description of the form [9], [39], [40]

$$M\dot{V}_{of} - ad^T_{V_{of}} M V_{of} = F_m + G + A^T\lambda \tag{25}$$

where for $V_{of} = (v^T, w^T)^T \in \mathbb{R}^6$

$$ad_{V_{of}} = \begin{bmatrix} \hat{w} & \hat{v} \\ 0 & \hat{w} \end{bmatrix}$$

is the adjoint map associated with V_{of}. By inverting Montana's equations of contact, V_{of} can be expressed in terms of $\dot{\eta}$ as

$$V_{of} = \begin{bmatrix} R_\psi M_o & -M_f & 0 \\ 0 & 0 & 0 \\ R_\psi R_o K_o M_o & -R_o K_f M_f & 0 \\ -T_o M_o & -T_f M_f & 1 \end{bmatrix} \begin{bmatrix} \dot{\alpha}_o \\ \dot{\alpha}_f \\ \dot{\psi} \end{bmatrix} := J\dot{\eta} \tag{26}$$

where

$$R_\psi = \begin{bmatrix} \cos\psi & -\sin\psi \\ -\sin\psi & -\cos\psi \end{bmatrix} \quad \text{and} \quad R_o = \begin{bmatrix} 0 & -1 \\ 1 & 0 \end{bmatrix}.$$

Substituting (26) into (25) yields

$$MJ\ddot{\eta} + C_1 = F_m + G + A^T\lambda \tag{27}$$

where $C_1 = M\dot{J}\dot{\eta} - ad^T_{J\dot{\eta}} MJ\dot{\eta}$. Decoupling the above equation using P_w and $I - P_w$ gives

$$\tilde{M}\ddot{\eta} + \tilde{C}_1 = B_1 F_m + B_1 G$$

and

$$-\phi_3 - \lambda = b_2 F_m + b_2 G$$

where

$$\tilde{M} = \begin{bmatrix} m\rho\cos\psi & -m\rho\sin\psi\cos u_o & -m & 0 & 0 \\ -m\rho\sin\psi & -m\rho\cos\psi\cos u_o & 0 & -m & 0 \\ -I_x\sin\psi & -I_x\cos u_o\cos\psi & 0 & 0 & 0 \\ -I_y\cos\psi & I_y\cos u_o\sin\psi & 0 & 0 & 0 \\ 0 & -I_z\sin u_o & 0 & 0 & I_z \end{bmatrix}$$

$$\tilde{C}_1 = [\beta_1 - \phi_1 \quad \beta_2 - \phi_2 \quad \beta_4 - \phi_4 \quad \beta_5 - \phi_5 \quad \beta_6 - \phi_6]^T$$

$$B_1 = \begin{bmatrix} 1 & 0 & 0 & 0 & 0 & 0 \\ 0 & 1 & 0 & 0 & 0 & 0 \\ 0 & 0 & 0 & 1 & 0 & 0 \\ 0 & 0 & 0 & 0 & 1 & 0 \\ 0 & 0 & 0 & 0 & 0 & 1 \end{bmatrix}$$

$$b_2 = [0 \quad 0 \quad 1 \quad 0 \quad 0 \quad 0]$$

and

$$\begin{aligned}
\beta_1 =& m\left(-\rho\sin\psi\dot{\psi}\dot{u}_o - \rho\cos\psi\cos u_o\dot{\psi}\dot{v}_o + \rho\sin\psi\sin u_o\dot{u}_o\dot{v}_o\right) \\
\beta_2 =& m\left(-\rho\cos\psi\dot{\psi}\dot{u}_o + \rho\sin\psi\cos u_o\dot{\psi}\dot{v}_o + \rho\cos\psi\sin u_o\dot{u}_o\dot{v}_o\right) \\
\beta_4 =& I_x\left(-\cos\psi\dot{u}_o\dot{\psi} + \cos u_o\sin\psi\dot{\psi}\dot{v}_o + \sin u_o\cos\psi\dot{u}_o\dot{v}_o\right) \\
\beta_5 =& I_y\left(\sin\psi\dot{u}_o\dot{\psi} + \cos u_o\cos\psi\dot{\psi}\dot{v}_o - \sin u_o\sin\psi\dot{u}_o\dot{v}_o\right) \\
\beta_6 =& -I_z\cos u_o\dot{u}_o\dot{v}_o \\
\phi_1 =& m\zeta_1\zeta_2 \\
\phi_2 =& m\zeta_1\zeta_3 \\
\phi_3 =& m\zeta_4\zeta_3 + m\zeta_5\zeta_2 \\
\phi_4 =& (I_z - I_y)\,\zeta_4\zeta_1 \\
\phi_5 =& (I_x - I_z)\,\zeta_5\zeta_1 \\
\phi_6 =& (I_x - I_y)\,\zeta_5\zeta_4 \\
\zeta_1 =& \sin u_o\dot{v}_o - \dot{\psi} \\
\zeta_2 =& \rho\sin\psi\dot{u}_o + \rho\cos\psi\cos u_o\dot{v}_o + \dot{v}_f \\
\zeta_3 =& \rho\cos\psi\dot{u}_o - \rho\sin\psi\cos u_o\dot{v}_o - \dot{u}_f \\
\zeta_4 =& -\cos\psi\dot{u}_o + \cos u_o\sin\psi\dot{v}_o \\
\zeta_5 =& -\sin\psi\dot{u}_o - \cos u_o\cos\psi\dot{v}_o.
\end{aligned}$$

The components of the Cartesian driving force F_m are designed as

$$\hat{F} = \tilde{M}\left(\ddot{\eta}_d - K_v\dot{\tilde{e}} - K_p\tilde{e}\right) + \tilde{C}_1 - B_1 G \tag{28}$$

$$f_3 = -\phi_3 - \lambda_d + K_I\int(\lambda - \lambda_d) - b_2 G \tag{29}$$

where $\alpha_{fd}(t) = 0$ to ensure that the end-effector stays normal to the sphere. $\hat{F} = [f_1, f_2, f_4, f_5, f_6]^T$. Let J_s be the Jacobian matrix of the manipulator. The corresponding joint torque is given by

$$\tau = J_s^T F_m. \tag{30}$$

The control diagram is shown in Fig. 7. In the experiment, we implemented the control law (28) and (29) in a testbed that consists of a six-DOF MOTORMAN robot, two Motorola 68 040 processors, a SUN workstation, and a six-DOF force/torque sensor. Force/torque data is sampled every 1 ms (1000 Hz) using an *A/D* board. A tactile sensor attached to the end-effector is used to detect the contact coordinate α_f and its velocity $\dot{\alpha}_f$. We

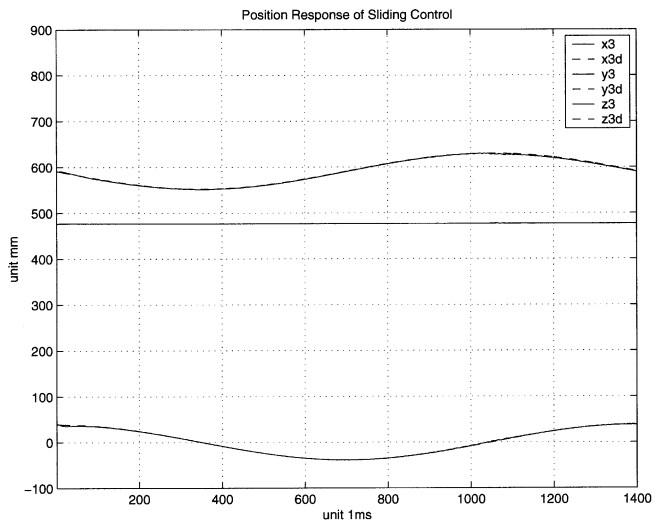

(a)

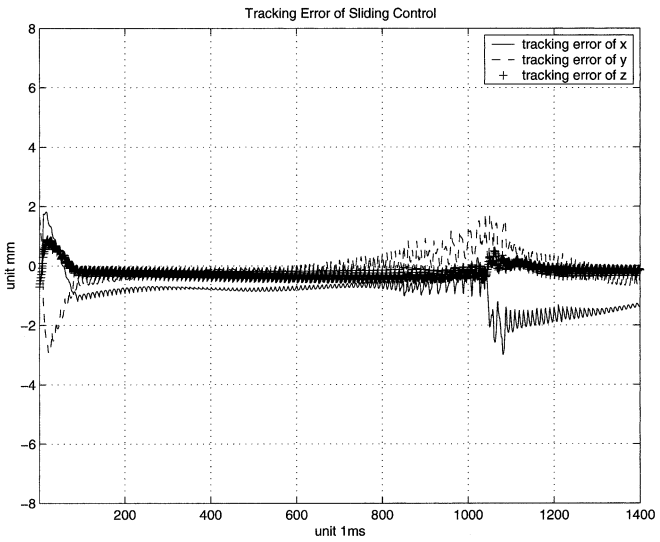

(b)

Fig. 8. (a) Position response. (b) Tracking error.

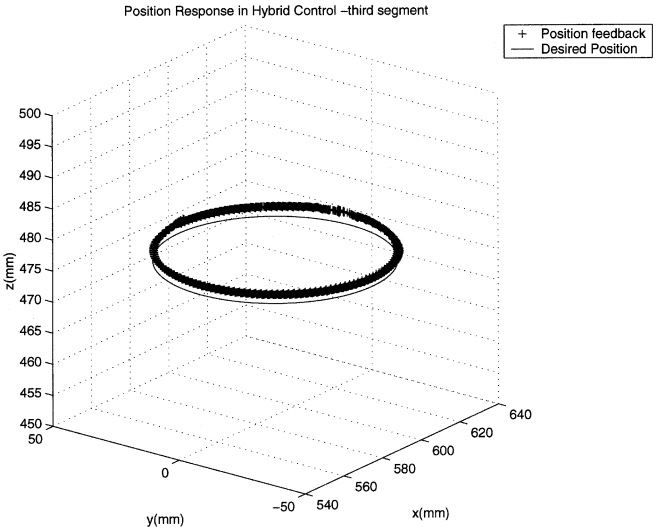

(a)

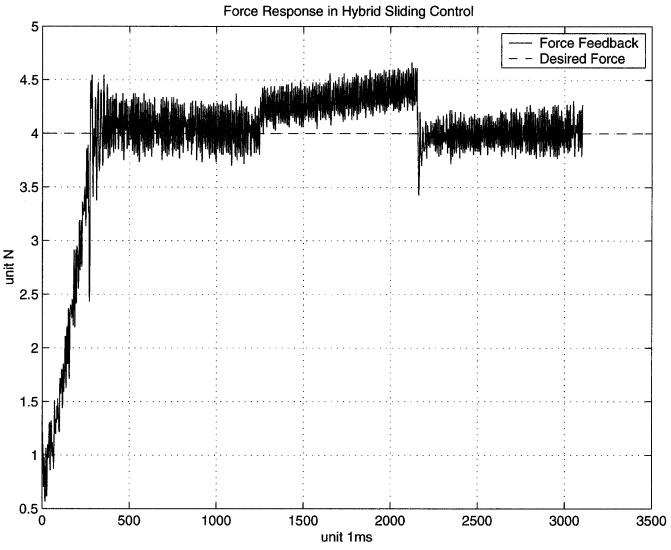

(b)

Fig. 9. (a) Three-dimensional view of the trajectory. (b) Force response.

used the following parameters in the experiment: $m = 0.91$ kg, $I_x = I_y = 0.0025\ \text{kg} \cdot \text{m}^2$, $I_z = 0.005\ \text{kg} \cdot \text{m}^2$, $\rho = 125$ mm, $K_p = \text{diag}(10, 10, 10, 10, 10)$, $K_v = \text{diag}(5, 5, 5, 5, 5)$, and $K_I = 0.02$. Figs. 8 and 9(a) show the position response and Fig. 9(b) the force response. Figs. 10 and 11 show the successive motion states of the manipulator sliding on a horizontal circle of the sphere.

Example 4: A Six-DOF Manipulator Rolling on a Sphere: In the previous example, let the contact constraint be pure rolling motion. Expressed in terms of the velocities of the local frames, these constraints are given by

$$\begin{bmatrix} 1 & 0 & 0 & 0 & 0 & 0 \\ 0 & 1 & 0 & 0 & 0 & 0 \\ 0 & 0 & 1 & 0 & 0 & 0 \\ 0 & 0 & 0 & 0 & 0 & 1 \end{bmatrix} \begin{bmatrix} v_x \\ v_y \\ v_z \\ w_x \\ w_y \\ w_z \end{bmatrix} := A_1 V_{l_o l_f} = 0$$

the constraint forces are of the form

$$f_c = A_1^T \lambda$$

where $\lambda \in \mathbb{R}^4$ lies in the friction cone defined by a soft finger contact [9]. Expressing rolling constraint in terms of V_{of}, we have

$$A_1 Ad_{g_{fl_f}^{-1}} V_{of} := A V_{of} = 0. \tag{31}$$

Rolling velocities in terms of $\dot{\alpha}_f$ are obtained by inverting Montana's equations of contact

$$\begin{bmatrix} w_x \\ w_y \end{bmatrix} = -R_o \left(K_f + R_\psi K_o R_\psi \right) M_f \dot{\alpha}_f.$$

Fig. 10. Successive motion states of sliding-first segment.

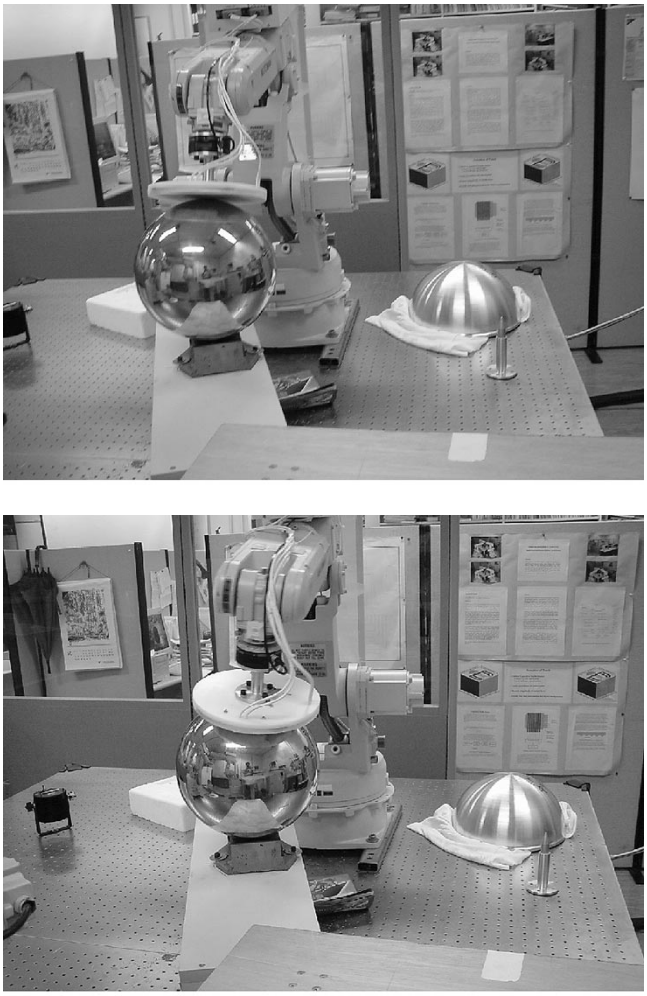

Fig. 11. Successive motion states of sliding-second segment.

Thus, the velocity of the end-effector in terms of $\dot{\alpha}_f$ is given by

$$\begin{aligned} V_{of} =& Ad_{g_{fl_f}} V_{l_o l_f} \\ =& Ad_{g_{fl_f}} \begin{bmatrix} 0 \\ 0 \\ 0 \\ -R_o \left(K_f + R_\psi K_o R_\psi\right) M_f \\ 0 \end{bmatrix} \dot{\alpha}_f \\ :=& J_f \dot{\alpha}_f. \end{aligned} \tag{32}$$

It can be shown that the tangent vector fields spanned by the columns of J_f is not involutive and thus, the constraints in (31) are nonholonomic. Substituting $V_{of} = J_f \dot{\alpha}_f$ into (25) yields

$$MJ_f \ddot{\alpha}_f + \left(M\dot{J}_f \dot{\alpha}_f - ad^T_{J_f \dot{\alpha}_f} M J_f \dot{\alpha}_f\right) = F_m + G + A^T \lambda \tag{33}$$

where $\lambda \in FC$. The hybrid velocity/force controller is designed as

$$\begin{aligned} F_m =& MJ_f \left(\ddot{\alpha}_{fd} - K_p \left(\dot{\alpha}_f - \dot{\alpha}_{fd}\right)\right) \\ &+ \left(M\dot{J}_f \dot{\alpha}_f - ad^T_{J_f \dot{\alpha}_f} M J_f \dot{\alpha}_f\right) \\ &+ A^T \left(-\lambda_d + \int \left(\lambda - \lambda_d\right)\right) - G. \end{aligned} \tag{34}$$

Note that the control law in (34) is similar to (28) and (29). However, only hybrid velocity/force control can be realized, as (32) is a local representation of the two-dimensional (2-D) distribution defined by the constraints (31). For velocity planning, we use $\dot{\alpha}_{fd} = J_f^{-1} V_{ofd}$ and $\ddot{\alpha}_{fd} = J_f^{-1} \dot{V}_{ofd} + \dot{J}_f^{-1} V_{ofd}$.

Fig. 12 shows the tracking result of the contact coordinates $\alpha_f(t)$, and Fig. 13(a) the 2-D view of the contact trajectory on the fingertip. Figs. 13(b) and 14 show the contact force response of λ_1, λ_2, and λ_3, respectively. The contact force λ_4 is hard to control due to the complex property of torsional friction. Fig. 15 shows the continuous motion states of the manipulator rolling on the sphere.

Example 5: Redundant Parallel Manipulator: Redundant constraints and actuation have been found to be effective means for removing singularities and improving performance of parallel manipulators [41]. Fig. 16 shows a two-DOF parallel planar manipulator with over constraint and over actuation. The ambient space E of the system is the 6–D torus $\mathcal{T}^6 = \mathbb{S}^1 \times \cdots \times \mathbb{S}^1$, parameterized by $\theta = (\theta_1, \ldots, \theta_6)^T$, where $(\theta_1, \theta_3, \theta_5)^T$ are actuated and $(\theta_2, \theta_4, \theta_6)^T$ are passive. Assuming equal link lengths for all chains, the four closure constraints of the manipulator are given by

$$\begin{bmatrix} x_a + lc_1 + lc_{12} - x_b - lc_3 - lc_{34} \\ y_a + ls_1 + ls_{12} - y_b - ls_3 - ls_{34} \\ x_a + lc_1 + lc_{12} - x_c - lc_5 - lc_{56} \\ y_a + ls_1 + ls_{12} - y_c - ls_5 - ls_{56} \end{bmatrix} := H(\theta) = 0$$

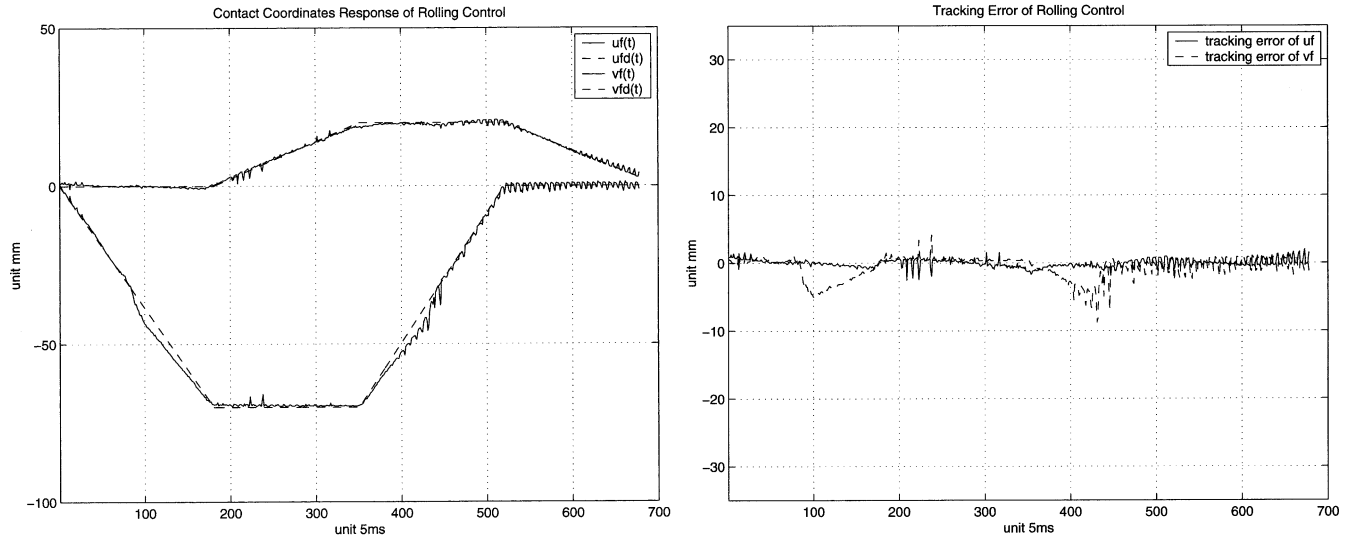

(a) (b)

Fig. 12. (a) Contact coordinates response. (b) Tracking error.

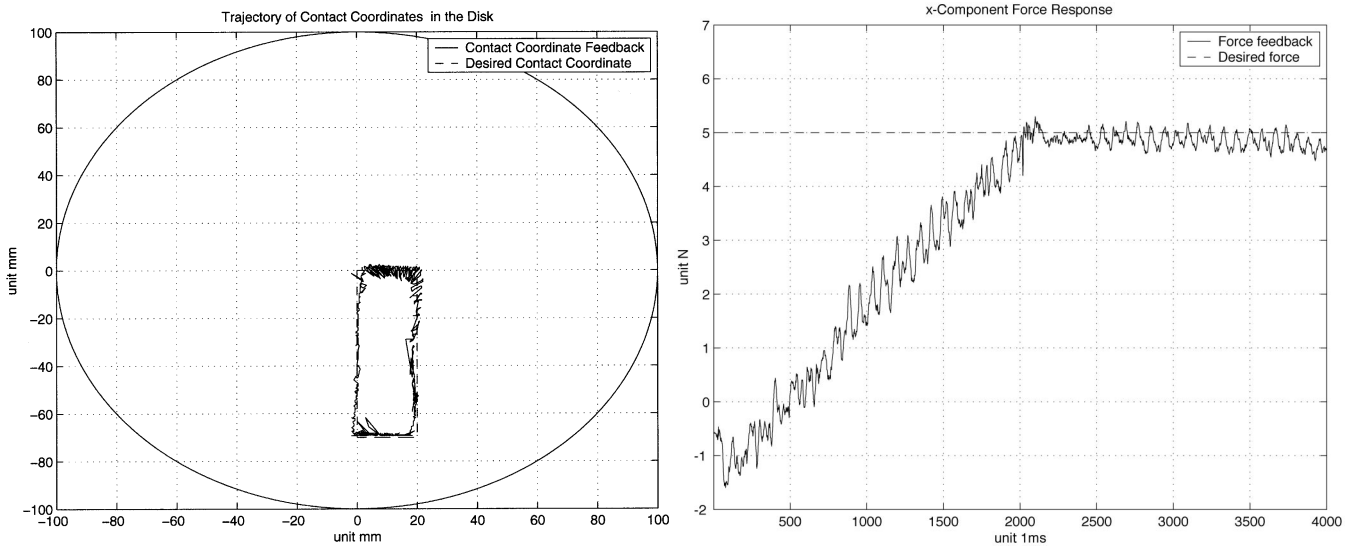

(a) (b)

Fig. 13. (a) 2–D view of contact trajectory on the fingertip. (b) Response of contact force λ_1.

where $c_i = \cos\theta_i$, $c_{ij} = \cos(\theta_i + \theta_j)$, $s_i = \sin\theta_i$, and $s_{ij} = \sin(\theta_i + \theta_j)$. Differentiating the closure constraints yields the velocity constraints as shown in (35) at the bottom of the page. If the constraint in (35) is linearly independent, it defines a 2–D configuration space $Q = H^{-1}(0)$. Q can be locally parameterized by any combinations of two actuated joints, or the Cartesian coordinates (x, y) of the system. Overactuation provides a freedom in avoiding parameterization singularities. Let $M_i \in \mathbb{R}^{2\times 2}$, $i = 1, \ldots, 3$ be the inertia matrix of the ith chain and define $M(\theta) = \text{diag}(M_1, M_2, M_3) \in \mathbb{R}^{6\times 6}$. The equations of motion of the system have the form

$$M(\theta)\ddot{\theta} + C\left(\theta, \dot{\theta}\right) + N = \tau + A^T\lambda$$

where $A^T\lambda$, $\lambda \in \mathbb{R}^6$, can be interpreted as the internal "grasping" force. When the constraints in (35) are linearly independent, we can, in principle, design a stable hybrid control

$$\begin{bmatrix} -s_1 - s_{12} & -s_{12} & s_3 + s_{34} & s_{34} & 0 & 0 \\ c_1 + c_{12} & c_{12} & -c_3 - c_{34} & -c_{34} & 0 & 0 \\ -s_1 - s_{12} & -s_{12} & 0 & 0 & s_5 + s_{56} & s_{56} \\ c_1 + c_{12} & c_{12} & 0 & 0 & -c_5 - c_{56} & -c_{56} \end{bmatrix} \dot{\theta} := A\dot{\theta} = 0 \tag{35}$$

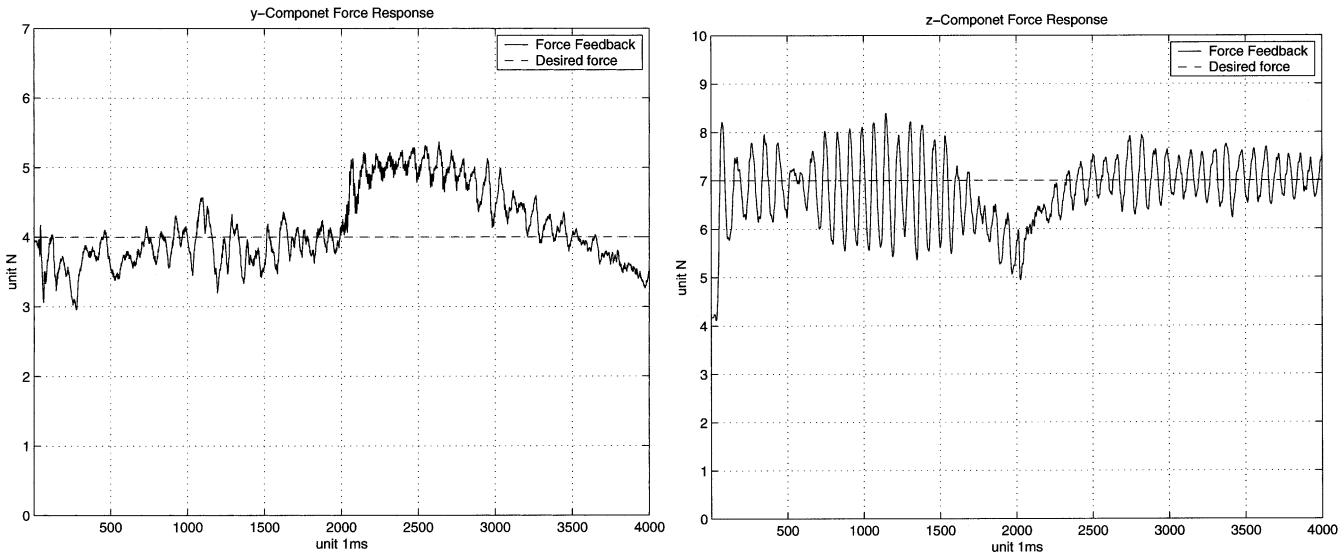

(a) (b)

Fig. 14. (a) Response of contact force λ_2. (b) Response of contact force λ_3.

Fig. 15. Successive motion states of rolling.

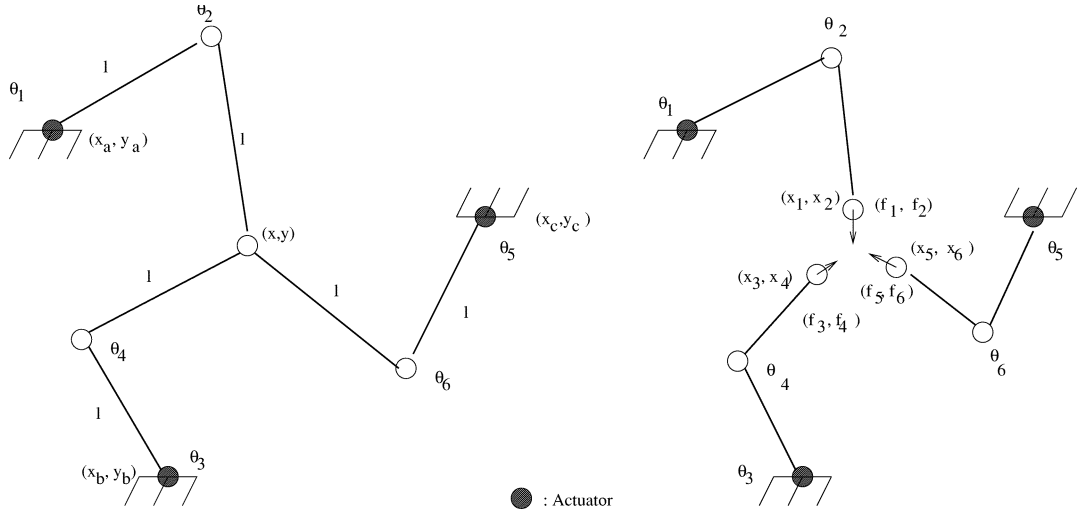

Fig. 16. Planar two-DOF parallel mechanisms with overactuation.

algorithm as in the previous examples to control the position of the end-effector and internal grasping force. However, since there are three unactuated joints, i.e., $\tau_2 = \tau_4 = \tau_6 = 0$, we can only achieve position control here. Let $\tilde{\theta} \in \mathbb{R}^2$ be a local parameterization of Q, $\theta = \psi(\tilde{\theta})$ an imbedding of Q in E, and $\dot{\theta} = J\dot{\tilde{\theta}}$ the differential of ψ. Define the projection map $P_w : T^*_\theta E \to T^*_\theta Q$ using M and A as in Section II. The projected dynamics in $T^*_\theta Q$ are given by

$$P_w M J\ddot{\tilde{\theta}} + P_w (C_1 + N) = P_w \tau \tag{36}$$

where $C_1 = M\dot{J}\dot{\tilde{\theta}} + C(\theta, J\dot{\tilde{\theta}})$. Let

$$\tilde{\tau} = (\tau_1, \tau_3, \tau_5)^T, \quad \text{and} \quad \hat{P}_w = [p_1, p_3, p_5]$$

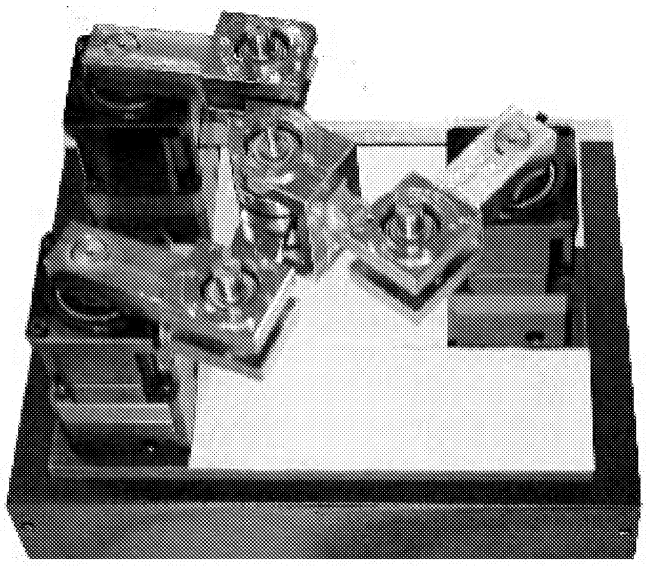

Fig. 17. System structure of two-DOF redundantly actuated parallel mechanism.

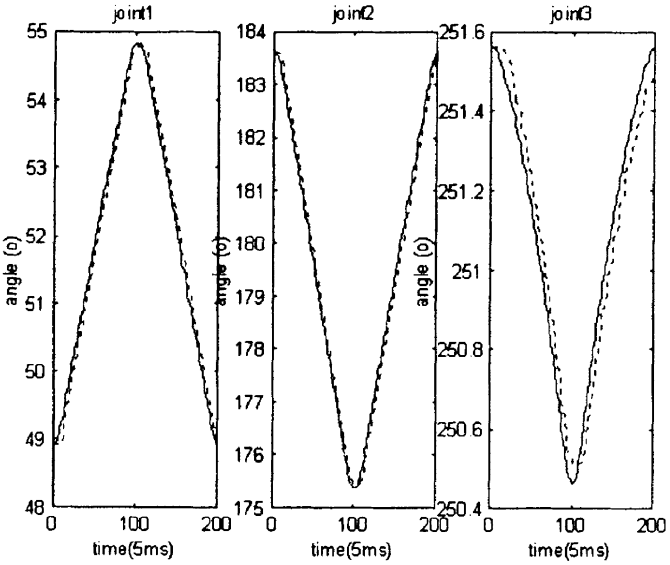

Fig. 18. Tracking results in joint space.

where p_i, $i = 1,3,5$, is the ith column of P_w. Let

$$\hat{\tau} = \hat{P}_w \tilde{\tau} = P_w \tau \in \mathbb{R}^6. \tag{37}$$

The control law for $\hat{\tau}$ in (36) which achieves asymptotic trajectory tracking of $\tilde{\theta}_d(t)$ is given by

$$\hat{\tau} = P_w M J \left(\ddot{\tilde{\theta}}_d - K_v \dot{\tilde{e}} - K_p \tilde{e} \right) + P_w \left(C_1 + N \right). \tag{38}$$

To see this, note that the closed-loop dynamics with (38) applied to (36) is of the form

$$P_w M J \left(\ddot{\tilde{e}} + K_v \dot{\tilde{e}} + K_p \tilde{e} \right) = 0.$$

Since Image$(J) = T_\theta Q$, $M(T_\theta Q) = T^*_\theta Q$, P_w is a projection map onto $T^*_\theta Q$, and $\eta(J) = \phi$, we conclude that

$$\ddot{\tilde{e}} + K_v \dot{\tilde{e}} + K_p \tilde{e} = 0.$$

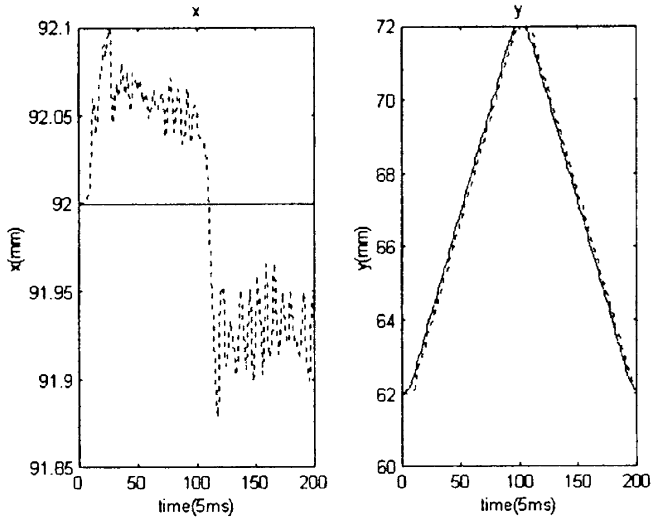

Fig. 19. Tracking results in Cartesian space.

Finally, given $\hat{\tau} \in T^*_\theta Q$, we need to solve for $\tilde{\tau}$ from (37). A sufficient condition for the existence of solution is that Image$(\hat{P}_w) = T^*_\theta Q$. This implies that a combination of three actuated joints can parameterize Q, i.e., absence of actuator singularities. In this case, minimal two-norm solutions can be used for $\tilde{\tau}$. Let $\tilde{\tau}_0 \in \eta(\hat{P}_w)$ and $\tilde{\tau}_1$ any solution such that $\hat{P}_w \tilde{\tau}_1 = \hat{\tau}$. Then

$$\tilde{\tau}_{\min} = \tilde{\tau}_1 + \hat{\gamma} \tilde{\tau}_0$$

where $\hat{\gamma} = -(\tilde{\tau}_0^T \tilde{\tau}_1)/(\tilde{\tau}_0^T \tilde{\tau}_0)$, is the optimal solution. We have realized minimal joint torque position control on the planar two-DOF parallel manipulator shown in Fig. 17. Figs. 18 and 19 show, respectively, the experimental results of the joint and end-effector space trajectories.

V. Conclusion

In this paper, we developed a unified geometric approach to the dynamic control of constrained mechanical systems. Starting from the constraint, we defined two natural subspaces, the free velocity space $T_\theta Q$ and the constraint force space $T^*_\theta Q^\perp$. Using the kinetic energy of the system, we also showed how to define the remaining subspaces and their relations under the $M^\sharp$ and $M^\flat$ maps. From the definition of these canonical subspaces, two projection maps naturally arise, which were subsequently used to obtain the projected dynamics of a constrained mechanical system, one in the constraint force space and another in its complement. Using the language of connections in Riemannian geometry, we provided an elegant interpretation of the constrained dynamics and explicitly showed the curvature effect on force control. Based on the geometric structure of the projected equations we proposed a stable hybrid position/force control algorithm for mechanical systems with holonomic constraints. We also showed that for nonholonomic systems hybrid velocity/force control can be achieved.

Several representative examples were worked out in detail to demonstrate the effectiveness of the hybrid control theory. Experimental results were also included in the case of a six-DOF

manipulator under end-effector constraints, both holonomic and nonholonomic. The proposed hybrid control theory was shown to be general enough to include applications such as closed-chain systems and multifingered robotic hands as well.

ACKNOWLEDGMENT

The authors would like to thank the unanimous reviewers for their useful suggestions during the revision of the paper.

REFERENCES

[1] M. T. Mason, "Compliance and force control for computer controlled manipulators," *IEEE Trans. Syst., Man, Cybern.*, vol. SMC-11, pp. 418–432, 1981.
[2] M. H. Raibert and J. J. Craig, "Hybrid position/force control of manipulators," *Trans. ASME J. Dynam. Syst., Meas., Contr.*, vol. 102, pp. 126–133, June 1981.
[3] K. Sugimoto and J. Duffy, "Application of linear algebra to screw system," *Mechanism Mach. Theory*, vol. 17, pp. 73–83, 1985.
[4] J. Duffy, "The fallacy of modern hybrid control theory that is based on orthogonal complements of twists and wrench spaces," *J. Robot. Syst.*, vol. 7, no. 2, pp. 139–144, 1990.
[5] J. Loncaric, "Geometric analysis of compliant mechanism in robotics," Ph.D. dissertation, Div. Appl. Sci., Harvard Univ., Cambridge, MA, 1985.
[6] K. H. Hunt, *Kinematic Geometry of Mechanisms*. London, U. K.: Oxford Univ. Press, 1978.
[7] R. S. Ball, *A Treatise on the Theory of Screws*. London, U. K.: Cambridge Univ. Press, 1900.
[8] J. Duffy, *Analysis of Mechanisms and Robot Manipulators*. London, U. K.: E. Arnold, 1980.
[9] R. Murray, Z. X. Li, and S. Sastry, *A Mathematical Introduction to Robotic Manipulation*. Boca Raton, FL: CRC, 1994.
[10] T. Yoshikawa, "Dynamic hybrid position/force control of robot manipulators—Description of hand constrains and calculation of joint driving force," *IEEE J. Robot. Automat.*, vol. RA-3, Oct. 1987.
[11] N. H. McClamroch and D. W. Wang, "Feedback stabilization and tracking of constrained robots," *IEEE Trans. Automat. Contr.*, vol. 33, pp. 419–426, May 1988.
[12] J. M. Selig, "Curvature in force/position control," in *Proc. IEEE Int. Conf. Robotics Automation*, 1998, pp. 1761–1766.
[13] A. De Luca, C. Manes, and G. Ulivi, "Robust hybrid dynamic control of robot arms," in *Proc. 28th Conf. Decision and Control*, vol. 1989, pp. 2641–2646.
[14] X. P. Yun and N. Sarkar, "Unified formulation of robotic systems with holonomic and nonholonomic constraints," *IEEE Trans. Robot. Automat.*, vol. 14, pp. 640–650, Aug. 1998.
[15] W. Blajer, "A geometric unification of constrained system dynamics," *Multibody Syst. Dynam.*, vol. 1, pp. 3–21, 1997.
[16] ——, "A geometrical interpretation and uniform matrix formulation of multibody system dynamics," *Zeitschrift fuer Angewandte Mathematik und Mechanik 81*, vol. 4, pp. 247–259, 2001.
[17] J. J. Murray and G. H. Lovell, "Dynamic modeling of closed-chain robotic manipulators and implications for trajectory control," *IEEE Trans. Robot. Automat.*, vol. 5, pp. 522–528, Aug. 1989.
[18] Y. Nakamura and M. Ghodoussi, "Dynamics computation of closed-link robot mechanisms with nonredundant and redundant actuators," *IEEE Trans. Robot. Automat.*, vol. 5, pp. 294–302, June 1989.
[19] A. Cole, J. Hauser, and S. Sastry, "Kinematics and control of a multifingered robot hand with rolling contact," *IEEE Trans. Automat. Contr.*, vol. 34, pp. 398–404, Apr. 1989.
[20] A. Cole, P. Hsu, and S. Sastry, "Dynamic control of sliding by robot hands for regrasping," *IEEE Trans. Robot. Automat.*, vol. 8, pp. 42–52, Feb. 1992.
[21] E. Paljug, X. Yun, and V. Kummar, "Control of rolling contacts in multi-arm manipulation," *IEEE Trans. Robot. Automat.*, vol. 10, pp. 441–452, Aug. 1994.
[22] N. Sarkar, X. P. Yun, and V. Kumar, "Dynamic control of 3-D rolling contacts in two-arm manipulation," *IEEE Trans. Robot. Automat.*, vol. 13, pp. 354–376, Aug. 1997.
[23] ——, "Control of contact interactions with acatastatic nonholonomic constraints," *Int. J. Robot. Res.*, vol. 16, no. 3, pp. 357–373, 1997.
[24] T. Yoshikawa, "Control algorithms for grasping and manipulation by multifingered robot hands using virtual truss model representation of internal force," in *Proc. IEEE Int. Conf. Robotics and Automation*, 2000, pp. 369–376.
[25] X. Z. Zheng, R. Nakashima, and T. Yoshikawa, "On dynamic control of finger sliding and object motion in manipulation with multifingered hands," *IEEE Trans. Robot. Automat.*, vol. 16, pp. 469–481, Oct. 2000.
[26] J. P. Ostrowski, "Computing reduced equations for mechanical systems with constraints and symmetries," *IEEE Trans. Robot. Automat.*, vol. 15, pp. 111–123, Feb. 1999.
[27] J. P. Ostrowski and J. W. Burdick, "The geometric mechanics of undulatory robotic locomotion," *Int. J. Robot. Res.*, vol. 17, no. 7, pp. 683–702, 1998.
[28] W. Boothby, *An Introduction to Differentiable Manifolds and Riemannian Geometry*. New York: Academic, 1975.
[29] J. E. Marsden and T. S. Ratiu, *Introduction to Mechanics and Symmetry*. New York: Springer-Verlag, 1994.
[30] Q. Lin and J. W. Burdick, "On well-defined kinematic metric functions," in *Proc. IEEE Int. Conf. Robotics and Automation*, 2000, pp. 170–177.
[31] M. Žefran, V. Kumar, and C. B. Croke, "On the generation of smooth three-dimensional rigid body motions," *IEEE Trans. Robot. Automat.*, vol. 14, pp. 576–589, Aug. 1998.
[32] R. M. Rosenberg, *Analytical Dynamics of Discrete Systems*. New York: Plenum, 1977.
[33] M. Griffis, C. Crane, and J. Duffy, "Displacements that null forces," in *Proc. IEEE Int. Symp. Intelligent Control*, Arlington, VA, 1991, pp. 110–115.
[34] J. Marsden and T. Ratiu, *Introduction to Mechanics and Symmetry*. New York: Springer-Verlag, 1994.
[35] F. Bullo, "Nonlinear control of mechanical systems: A Riemannian geometry," Ph.D. dissertation, Dept. Contr. Dynam. Syst., CA Inst. Technol., Pasadena, CA, 1999.
[36] C. Canudas, B. Siciliano, and G. Bastin, *Theory of Robot Control*. New York: Springer-Verlag, 1996.
[37] D. Montana, "The kinematics of contact and grasp," *Int. J. Robot. Res.*, vol. 7, no. 3, pp. 17–32, 1988.
[38] Z. Li and J. Canny, "Motion of two rigid bodies with rolling constraint," *IEEE Trans. Robot. Automat.*, vol. RA2-06, pp. 62–72, Feb. 1990.
[39] S. R. Ploen and F. Park, "Coordinate-invariant algorithms for robot dynamics," *IEEE Trans. Robot. Automat.*, vol. 15, pp. 1130–1135, Dec. 1999.
[40] J. M. Selig, *Geometrical Methods in Robotics*. New York: Springer-Verlag, 1996.
[41] J. F. O'Brien and J. T. Wen, "Redundant actuation for improving kinematic manipulability," in *Proc. IEEE Int. Conf. Robotics and Automation*, 1999, pp. 1520–1525.

Guanfeng Liu received the B.E. degree in electrical engineering from Zhejiang University, Hangzhou, China, in 1998. He is currently pursuing the Ph.D. degree at the Hong Kong University of Science and Technology, Kowloon.

His research interests include multifingered manipulation, parallel manipulators, and robotic locomotion.

Zexiang Li (M'83) received the B.S. degree in electrical engineering and economics (with honors) from Carnegie Mellon University, Pittsburgh, PA, in 1983 and the M.A. degree in mathematics and Ph.D. degree in electrical engineering and computer science, both from the University of California, Berkeley, in 1985 and 1989, respectively.

He is an Associate Professor with the Electrical and Electronic Engineering Department, Hong Kong University of Science and Technology, Kowloon. His research interests include robotics, nonlinear system theory, and manufacturing.